

# Noise Modeling for Design and Simulation of Color Imaging Systems

*Hans B. Wach and Edward R. Dowski, Jr.*  
*CDM Optics, Inc.*  
*Boulder, Colorado, USA*

## Abstract

Understanding signal and noise quantities in any practical color imaging system is critical. Often noise quantities are assumed to be independent of the signal, independent of color channel and either uniform or Gaussian additive. These simplistic models are not realistic and there is a need for accurate noise models in order to design optimal color imaging systems. Different noise characteristics between the individual color channels should be taken into account when developing demosaicing methods, noise reduction algorithms and other image processing tasks. The choice of color space in which to operate on a color image is also dependent on the noise characteristics of the sensor. It is also possible to optimize the filters in the CFA (color filter array) based on knowledge of the sensor noise. We describe a noise model for a modern APS CMOS detector and a number of noise sources. A method for characterizing the noise sources given a set of dark images and a set of flat field images is outlined. The noise characterization data is used to simulate dark images and flat field images. The simulated data is a very good match to the real data thus validating the model and characterization procedure.

## 1. Introduction

Noise models are determined by the type of detector as well as the physical nature of detectors within each class. We particularly consider models for modern, single sensor, three transistor (3T) APS CMOS detectors employing a CFA. Signal, temperature and time dependent noise sources are all present in a CMOS detector and must be modeled appropriately. Fixed pattern noise plays a large role in this noise model particularly due to its large signal-dependent component and its effect on demosaicing. Impulsive noise, due to dark current and random telegraph signal noise, is problematic as it too leads to unwanted color artifacts in the resulting image.

We first describe the noise model and describe the fixed pattern and temporal noise components. Both the temporal noise and the fixed pattern noise components have both signal dependent and signal independent quantities. With the noise model and understanding of the different noise sources, we offer techniques for estimating the noise sources.

The accuracy of the model is shown through simulations of simple noisy images with comparison actual images.

An important note should be made on characterizing noise for a single sensor versus a group of sensors. In the case of a single sensor, noise that varies as a function of spatial pixel location and does not change over time is termed FPN (fixed pattern noise). While this form of noise is deterministic, or fixed, for this one sensor from which it was measured, it is different for all other sensors. Although a family of sensors may have a deterministic component of fixed pattern noise that is dependent on the manufacturing process and the actual chip design and layout, we will be treating FPN as a random process from one sensor to the next. Since our purpose is to model noise in digital sensors we will be seeking a statistical understanding of the FPN for a group of sensors. For this reason we avoid the term *deterministic* in this paper and instead rely on the term *fixed pattern noise* to convey both the deterministic (fixed pattern) and statistical (noise) nature of the noise.

## 2. Noise Model

The noise model we are considering for 3T CMOS APS sensors is shown in Figure 1 and consists of common components.<sup>1,7</sup> Incoming photons are directed through a series of optical elements including lenses, lenslet arrays, IR filters and a CFA before impinging on the photosensitive area. Each pixel has a slightly different photoresponsivity due to differences in photosensitive area geometry denoted by  $G_{PRNU}$ . The uncertainty in the number of photons landing on the photosite due to shot noise is modeled as a Poisson process such that the variance of the shot noise is equal to the mean signal level. The current level  $i_{ph}$  is considered a deterministic quantity.

Each pixel generates a certain amount of dark current denoted by  $i_{dc}$ , which is integrated over the exposure time. The dark current has an associated shot noise modeled by the Poisson process. For each pixel comprising an image frame, the dark current, dark current shot noise, signal and photon shot noise are summed together before continuing through a chain of amplifiers.

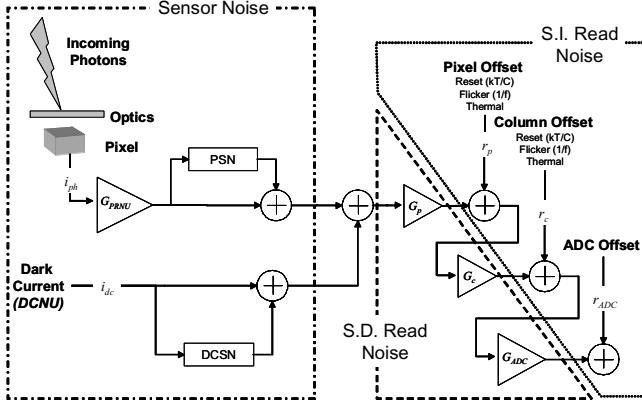


Figure 1. Block diagram of the noise model employed in this paper. Three categories of noise sources are segmented: Sensor Noise, Signal Independent (S.I.) Read Noise and Signal Dependent (S.D.) Read Noise..

Each pixel has its own conversion gain, denoted  $G_p$ , and a DC offset imposed by the amplifier,  $r_p$ . The DC offset has a component that appears as fixed pattern noise and a time varying component which is related to reset noise, flicker noise, and thermal noise, all of which will be described in Section 3. All pixels in a column share a common column amplifier. Similar to the pixel amplifiers, each column has its own gain,  $G_c$ , and associated DC offset,  $r_c$ , that has both a fixed pattern noise component and temporal noise component. Depending on the design of the sensor there may be one or more ADCs (in fact, some advanced technology sensors have an ADC for each pixel<sup>6</sup>). We model a system with a single ADC for each color channel. These three ADCs have potentially different gains and DC offsets associated with them and they are denoted  $G_{ADC}$  and  $r_{ADC}$  respectively.

### 3. Noise Sources

As is obvious from the preceding section and Figure 1, there are a number of noise sources to consider. In this section we will briefly outline these different noise sources, their origin, and their classification.<sup>7</sup> Referring to Figure 1, the noise sources bounded by the rectangle correspond to what we term *sensor noise*. All of these sources happen at the photoelectron level before any amplification. The sources bounded by a triangle correspond to *signal dependent read noise* (gain) and those bounded by the polygon correspond to *signal independent read noise* (offset). In Section 3.1 we will discuss the spatial noise sources, also termed fixed pattern noise (FPN) and in Section 3.2 we will cover the temporal noise sources. Finally in Section 3.3 we will discuss some simplifications and assumptions made in the noise modeling and measurement process.

#### 3.1 Fixed Pattern Noise

The first form of noise we consider is a variation in pixel photoresponsivity. That is, if a constant  $N$  photons fell

on each pixel we expect a variation in the number of electrons generated from those photons in the different pixels. This type of noise, termed photo response nonuniformity (PRNU), shows up as a signal dependent, fixed pattern noise. The underlying cause of this noise is attributed to differences in sense-node geometry (which results in differing capacitances).<sup>8</sup> PRNU is shown as a gain block labeled  $G_{PRNU}$  in Figure 1.

Another fixed pattern noise is dark current nonuniformity (DCNU). Each pixel has differing amounts of dark current and the resulting image will have DCNU noise that is linearly related to the exposure time and exponentially related to the temperature. Dark current nonuniformity is the fundamental limit of fixed pattern noise and can only be reduced by cooling of the sensor or better manufacturing control. However, its effect can be reduced by using short exposure times. Dark current nonuniformity is largely caused by impurities and defects in the silicon substrate. Newer CMOS designs, borrowing from CCD technology, are incorporating a pinned-photodiode structure. This 4T (four transistor) structure faces some fabrication challenges and some performance hindrances but offers a much reduced dark current and improved blue response.<sup>9, 10</sup>

Due to differences in the transistors for each pixel, there is a varying pixel gain across the sensor which contributes to fixed pattern noise. This FPN component we will refer to as pixel gain nonuniformity,  $G_p$ . While this is a signal dependent FPN source there is a FPN offset (signal independent) noise source,  $r_p$ , due to read noise associated with each pixel. However, the read noise is largely reduced by the use of correlated double sampling (CDS).<sup>1,2,5</sup>

All pixels in the same column share a column amplifier. Differences in the gain,  $G_c$ , and offset (read noise),  $r_c$ , of these amplifiers contribute to a column-wise fixed pattern noise. Some sensors incorporate double sampling of the column data as well as the pixel data. This second level of CDS, known as “crowbar”, significantly reduces the effect of the read and reset column noise.<sup>1,2</sup> The differences in column gain are very important to minimize (through careful manufacturing) as a failure to do so will result in a very obvious column-wise noise at all signal levels.

#### 3.2 Temporal Noise

Photon shot noise (PSN) derives from the uncertainty in the number of photons falling on an individual photosite. This type of noise is signal dependent and becomes more noticeable at higher signal levels. At low light levels, dark current shot noise (DCSN) can dominate. As discussed above, dark current can be lessened through better manufacturing, cooling of the sensor and more advanced pixel architectures. However, there is nothing that can be done to eliminate shot noise whether photon shot noise or dark current shot noise.

Pixel reset noise, also known as  $kT/C$  noise, comes from the uncertainty of the pixels reset level. Optimally, a reset pixel would have no charge on it, but this is not the case in reality. Reset noise can be canceled by the use of CDS at the pixel level. Other temporal noise sources at the pixel level

are flicker ( $1/f$ ) and thermal noise. While these two noise sources are inherent to MOS devices their effect can be minimized in CMOS sensors. Flicker noise can be largely reduced through the use of CDS and thermal noise can be reduced by minimizing the bandwidth of the pixel amplifiers.<sup>1,2,5,7</sup>

Similar to the temporal noise sources at the pixel level, the column amplifier circuits also have their share of noise. Again, reset, flicker and thermal noise sources are typically present with the largest contributor being the reset noise<sup>7</sup>. Column level CDS can significantly reduce the column reset noise.<sup>1,7</sup>

The analog to digital converter (ADC) is another source of temporal noise, with the primary component being quantization noise. There is also an offset associated with the ADC which should be considered for accurate modeling.

### 3.3 Assumptions and Simplifications

The two major components of signal dependent pixel fixed pattern noise (FPN) are the PRNU and pixel gain nonuniformity. The size of the photosensitive area is relatively large in CMOS APS sensors and can be manufactured to tight tolerances thus leading to very little FPN from PRNU.<sup>1</sup> In photogate sensors, a higher conversion gain can be attained by shrinking the capacitance of the floating diffusion node. While this reduced capacitance leads to a higher conversion gain, its small size makes uniform manufacturing difficult leading to higher conversion gain nonuniformity<sup>1</sup>. In this paper we will assume zero PRNU.

The fact that the sources of column and pixel FPN come from different device parameters leads to the assumption that the associated random processes are uncorrelated.<sup>3</sup> For this paper we will assume no inter-pixel correlation and no inter-column correlation. In general, this is a bad assumption but will suffice for a simple model. A better assumption is described in another paper<sup>3</sup> where both the pixel and column FPN are modeled as a first order isotropic autoregressive processes.

The photodiode capacitance is not constant (as is typically assumed) but rather a function of its reverse bias voltage thereby giving a nonlinear output voltage to a linear input current. The effect of the nonlinearity is only substantial at large signal levels.<sup>4</sup> Most of our characterization is done at zero, low and medium light levels and so we assume that the pixel photodiode capacitance remains constant during integration. We also assume a very simple read noise model. More in depth analysis of read noise can be found elsewhere.<sup>4</sup>

## 4. Noise Measurement and Characterization

We begin by describing the necessary data to be collected for noise measurement followed by an in depth look at characterizing the dark signal fixed pattern noise and temporal noise. The section concludes with further fixed pattern noise characterization with flat field signal data.

In order to measure the noise components of a sensor, two sets of images are taken: one set in the absence of light

and the other with flat field illumination. Each set of images is comprised of images from the full range of exposures with  $N$  images taken at each exposure level ( $N$  typically being greater than 20). We denote each image as:

$$I(i, j, k, t_{\text{exp}}) \quad (1)$$

where  $i$  and  $j$  are the spatial variables,  $t_{\text{exp}}$  is the exposure and  $k$  is a time index for each exposure that is in the range  $[0 N]$ . The set of dark signal images are used to extract a number of FPN components, some temporal noise components and is used to determine the sensor conversion gain and full well. The set of flat field images also reveals some FPN noise and also allows us to compute the optical sensitivity of the individual channels (differences are attributed to the color filter array).

### 4.1. Dark Signal: FPN Measurement and Simulation

#### A. Overall Dark Signal

The FPN components that can be determined from the dark signal data can be grouped into a slope component and an offset component. After acquiring a full set of dark images, a time averaged dark frame is computed for each exposure level,

$$\begin{aligned} F_{\text{dark}}(i, j, t_{\text{exp}}) &= \frac{1}{N} \sum_{k=0}^N I_{\text{dark}}(i, j, k, t_{\text{exp}}) \\ &= i_{\text{dc}}(i, j)G_p(i, j)G_c(i)G_{\text{ADC}}t_{\text{exp}} + \dots \\ &\quad \dots + r_p(i, j)G_c(i)G_{\text{ADC}} + r_c(i)G_{\text{ADC}} + r_{\text{ADC}} \end{aligned} \quad (2)$$

Notice that the dark images should have no  $i_{\text{ph}}$  component and the temporal averaging removes any temporal noise such as the dark current shot noise.

To uncover the FPN components of interest we must study  $F_{\text{dark}}$  as a function of exposure for each pixel ( $i$  and  $j$ ) and fit a straight line to the data. We will divide the fixed pattern noise into a slope component (exposure dependent) and an offset component (exposure independent), the latter of which comes from analyzing the third line in (2).

#### B. Offset (Exposure Independent) FPN

We begin by taking a look at the offset component of fixed pattern noise by analyzing the third line of (2). We can write the dark signal offset noise as,

$$F_{\text{dark}}(i, j, 0) = G_{\text{ADC}}G_c(i)r_p(i, j) + G_{\text{ADC}}r_c(i) + r_{\text{ADC}} \quad (3)$$

In order to characterize the pixel offset we take the mean of the standard deviation along the columns, the  $j$  direction, of (3),

$$\text{mean}(\text{std}_j(F_{\text{dark}}(i, j, 0))) = \mu_{G_c} \mu_{G_{\text{ADC}}} \sigma_{r_p} \cdot \quad (4)$$

This is a scaled version of the standard deviation of the pixel offset. Other than a row-wise component to the pixel offset, likely due to a changing ADC offset, the top plot in Figure 2 reveals a Gaussian offset distribution. In order to find the standard deviation of the column amplifier offsets

we take the standard deviation of the mean along the columns, the  $j$  direction, of (3),

$$\begin{aligned} \text{std}(\text{mean}_j(F_{\text{dark}}(i, j, 0))) &= \dots \\ &\dots \sqrt{(\sigma_{G_c} \mu_{G_{\text{ADC}}} \mu_{r_p})^2 + (\mu_{G_{\text{ADC}}} \sigma_{r_c})^2} \end{aligned} \quad (5)$$

It is not possible to decouple the column offset deviation from the column gain deviation in (5), however, a good sensor will have well matched column gains to avoid column-wise noise at higher signal levels. Therefore, if we assume very small column gain deviation,  $\sigma_{G_c}$ , (5) can be simplified to,

$$\text{std}(\text{mean}_j(F_{\text{dark}}(i, j, 0))) \approx \mu_{G_{\text{ADC}}} \sigma_{r_c} \quad (6)$$

which is a scaled version of the column offset standard deviation. The bottom plot of Figure 2 shows the relative column offsets as a function of column index. The column offsets are also Gaussian distributed.

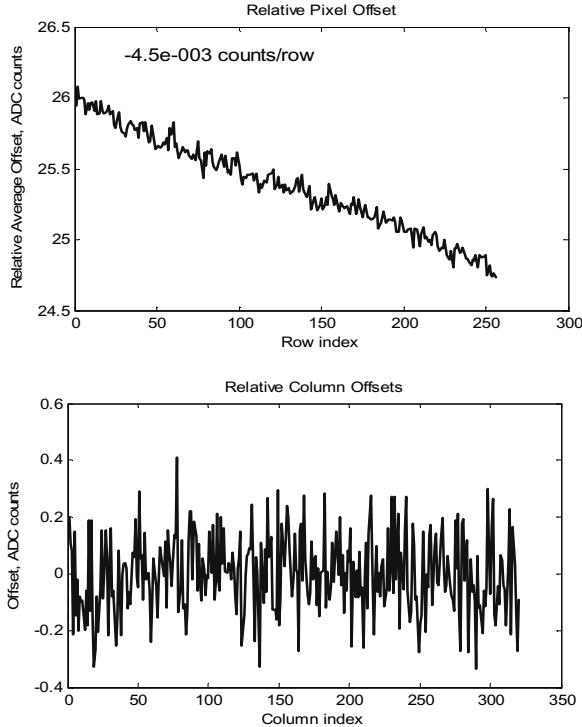


Figure 2. The upper plot shows a noticeable,  $-4.5e-3$  counts per row, row-wise component of pixel offset. This may be due to a change in ADC offset as a function of readout row. The lower plot shows the Gaussian distributed column-wise offset.

### C. Slope (Exposure Dependent) FPN

Returning to the second line of (2) we now examine the dark signal slope fixed pattern noise, or exposure dependent FPN. There are several components of this type of FPN, namely dark current nonuniformity and differences in pixel, column and ADC gains. It is our goal, in this section, to

determine the individual contributions of each of these components to the overall slope FPN. Again,  $G_{\text{ADC}}$  is assumed spatially constant and we compute the derivative of  $F_{\text{dark}}$  with respect to  $t_{\text{exp}}$  to obtain,

$$\dot{F}_{\text{dark}}(i, j) = \frac{d}{dt_{\text{exp}}} F_{\text{dark}}(i, j) = i_{\text{dc}}(i, j) G_p(i, j) G_c(i) \quad (7)$$

Reliably decoupling these three quantities (the dark current, pixel gains and column gains) is difficult at this point mainly because dark current of the sensor is not normally distributed and instead has extremely long tails due to a number of pixels with abnormally high dark current. Therefore it is difficult to discern the amount of deviation due to the column gains and the amount of deviation due to pixels with wild dark current. Later, using the flat field data, we will acquire a good estimate of the column gains and pixel gains and use that to extract the DCNU from (7).

### 4.2. Dark Signal: Temporal Noise Measurement and Simulation

The next step in characterizing the sensor is to measure the temporal noise by calculating the standard deviation of each pixel for a given exposure,

$$\sigma_{k, \text{dark}}(i, j, t_{\text{exp}}) = \sqrt{\frac{1}{N} \sum_{k=0}^{N-1} (I(i, j, k, t_{\text{exp}}) - F_{\text{dark}}(i, j, t_{\text{exp}}))^2} \quad (8)$$

Again we focus on a single color plane. The temporal noise is made up of dark current shot noise and read noise (including reset noise and thermal noise from pixel and column amplifiers) that add in quadrature

$$\sigma_k = \sqrt{\sigma_{\text{read}}^2 + \sigma_{\text{darkshot}}^2} \quad (9)$$

There should be zero dark current shot noise at zero exposure and this should increase with increasing exposure while the read noise is independent of exposure. The read noise, therefore, is,

$$\sigma_{\text{read}} = \sigma_{k, \text{dark}}(i, j, 0) \quad (10)$$

and the dark current shot noise can then be isolated from (9).

Using the well know square root relationship between dark current shot noise and the mean dark signal ( $\mu_{\text{dark}}$ ) the conversion gain,  $G_{\text{conv}}$  (in units of ADC counts per electron), of the sensor can be computed. That is, since the dark current shot noise obeys the Poisson statistic we can write,

$$\left( \frac{\sigma_{\text{darkshot}}}{G_{\text{conv}}} \right)^2 = \frac{\mu_{\text{dark}}}{G_{\text{conv}}} \rightarrow G_{\text{conv}} = \frac{\sigma_{\text{darkshot}}^2}{\mu_{\text{dark}}} \quad (11)$$

$$\text{where } \mu_{\text{dark}}(t_{\text{exp}}) = \text{mean}_{i, j}(F_{\text{dark}}(i, j, t_{\text{exp}}))$$

It is important to subtract the offset of the mean dark signal,  $\mu_{\text{dark}}(0)$ , from the total dark signal when acquiring the conversion gain. The conversion gain is the product of the pixel gain,  $G_p$ , the column gain,  $G_c$ , and the ADC gain,  $G_{\text{ADC}}$ . Given the conversion gain and the bit depth of the sensor one can determine the full well of the sensor by,

$$fullwell = \frac{2^{n_{bd}}}{G_{conv}}. \quad (12)$$

### 4.3. Flat Field Signal: FPN Measurement and Simulation

In the preceding sections we characterized a number of noise sources from dark signal data. Recall in Section 4.1.C that we could not get a good measure of the column gain deviation because it was intertwined with the dark current nonuniformity. Next we use flat field data (achieved by uniform illumination of the sensor) to better characterize the column gains. With this we can also uncover the pixel gains and the dark current nonuniformity.

The next set of data to be collected is a set of flat field images at varying exposures (ideally at the same exposures used when acquiring dark signal data). Again, at each exposure  $N$  images are taken and these  $N$  images are averaged together to remove temporal noise. If a true white light source is used for illumination then the optical sensitivity of each color channel can be found. The optical sensitivity is a function, mainly, of the CFA spectra and the microlenses and their alignment. Differences in optical sensitivity due to the CFA appear as a periodic FPN. We remove the effect of this by looking at each color channel independently. We do not compensate for the effects from the microlenses but these are relatively small compared to the effect from the CFA.

If the same exposures used during dark signal data collection are used for FF signal data collection, we can subtract the already measured dark data from the collected data. We will call this data set  $F_{ff-dark}$ . Because the data is from flat field illumination  $i_{ph}$  can be assumed constant. Recalling our assumption made in Section 3.3 we assume that  $G_{PRNU}$  is constant, thus the quantity  $m=i_{ph}G_{PRNU}$  is also constant. Taking the derivative of  $F_{ff-dark}$  with respect to  $t_{exp}$  we get,

$$\dot{F}_{ff-dark}(i, j) = mG_p(i, j)G_c(i) \quad (13)$$

From (13) it is now possible to isolate the column gain deviation and pixel gain deviation. By averaging down the columns of (13) and dividing  $\dot{F}_{ff-dark}(i, j)$  by the mean of  $\dot{F}_{ff-dark}(i, j)$  over  $i$  and  $j$  we get measure of the deviation of the column gain assuming a mean column gain of 1. That is,

$$\hat{G}_c(i) = \frac{G_c(i)}{\mu_{G_c}} = \frac{1}{hm\mu_p\mu_{G_c}} \sum_{j=0}^{h-1} \dot{F}_{ff-dark}(i, j) \quad (14)$$

Now, the relative column gains can be divided out of (13) in order to reveal a scaled version of the pixel gain,

$$\hat{G}_p(i, j) = \frac{\dot{F}_{ff-dark}(i, j)}{\hat{G}_c(i)} = \mu_{G_c} i_{ph} G_{PRNU} G_p(i, j) \quad (15)$$

Similarly, we can divide the relative column gains out of (7) and divide the result by (15) to reveal an estimate of the dark current,

$$\hat{i}_{dc}(i, j) = \frac{\dot{F}_{dark}(i, j)}{\hat{G}_c(i)\hat{G}_p(i, j)} = \frac{i_{dc}(i, j)}{i_{ph}G_{PRNU}} \quad (16)$$

The histogram of the dark current is shown in Figure 3. Notice the long tail of the distribution and the asymmetry. For simplicity, currently we assume a Gaussian dark current distribution in our simulations. The relative pixel gain distribution and relative column gain distribution are found to be Gaussian.

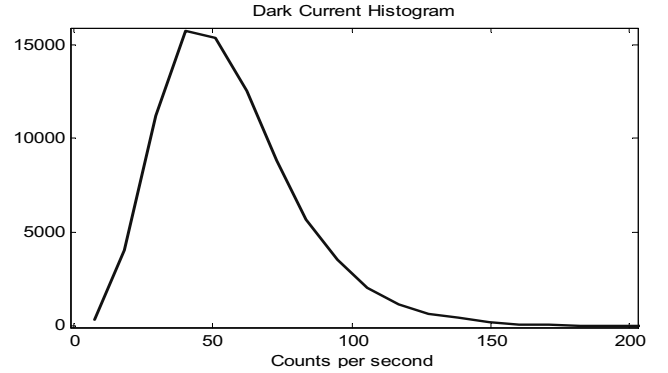


Figure 3. The dark current histograms for the individual channel. Notice the long tails on the distributions and the asymmetry.

### 4.4. Simulation Results

Once a sensor has been characterized as described in the preceding sections it is a relatively straight forward task to implement the model shown in Figure 1. Comparing results from the simulated data and the measured data it is nearly impossible to tell the difference.

Figure 4 shows the results of time averaged images at zero (top) and 60 millisecond (bottom) exposures for a single channel. A reversed colormap is used to avoid dark images caused by a few very high valued pixels. The flat field data is also simulated and the results are very close to the actual data.

## 5. Conclusion

We described a noise model for a particular sensor design and outlined a strategy for measuring and characterizing a number of noise sources. The model contained both temporal noise sources and spatial noise sources (fixed pattern noise). The noise sources were classified as either signal dependent or signal independent and whether or not they were exposure dependent. Although a number of simplifications and assumptions were made simulated images are shown for both dark field and flat field images and the results are very close to the actual data. With such accurate sensor simulations now available, it is now possible to simulate and optimize the whole optical-digital imaging system from optics, color filter array, choice of operating color space and image processing.

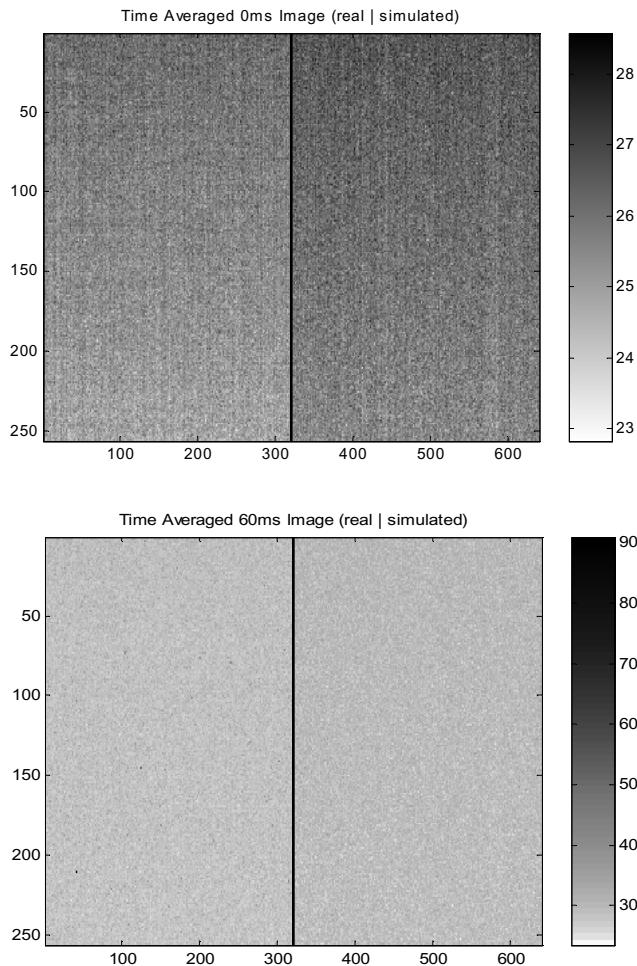


Figure 4. Time averaged, 0 ms exposure, dark images shown on top for both real data (on the left) and simulated data (on the right). On the bottom, time averaged, 60 ms exposure, dark images shown for the real data (on the left) and the simulated data (on the right). Notice the reversed colormap.

## References

1. Andrew J. Blanksby and Marc J. Loinaz, "Performance analysis of a color CMOS photogate sensor," *IEEE Trans. Electron Devices*, vol. 47, no. 1, pp. 55-64, Jan. 2000.
2. S. Mendis, S. Kemeny, R. Gee, B. Pain, C. Staller, Q. Kim, E. Fossum, "CMOS active pixel image sensors for highly integrated imaging systems," *IEEE J. Solid-State Circuits*, vol. 32, no. 2, pp. 187-197, Feb. 1997.
3. A. El Gamal, B. Fowler, H. Min, X. Liu, "Modeling and estimation of FPN components in CMOS image sensors," in *Proceedings of SPIE*, vol. 3301, (San Jose, CA), Jan. 1998.
4. H. Tian, B. Fowler, A. El Gamal, "Analysis of temporal noise in CMOS photodiode active pixel sensor," *IEEE J. Solid-State Circuits*, vol. 36, no. 1, pp. 92-101, Jan. 2001.
5. Albert Theuwissen and Edwin Roks, "Building a better mousetrap: Modified CMOS processes improve image sensor performance," *SPIE's OE Magazine*, pp. 29-32, Jan. 2001.
6. S. Kleinfelder, S. H. Lim, X. Liu and A. El Gamal, "A 10,000 frames/s CMOS digital pixel sensor," *IEEE J. Solid-State Circuits*, vol. 36, no. 12, pp. 2049-59, Dec. 2001.
7. Hewlett-Packard Components Group, "Noise sources in CMOS image sensors," [http://www.stw.tu-ilmeneau.de/~ff/beruf\\_cc/cmos/cmos\\_noise.pdf](http://www.stw.tu-ilmeneau.de/~ff/beruf_cc/cmos/cmos_noise.pdf), Jan. 1998.
8. Sandor L. Barna, "Sensors support low-light imaging," *Photonics Spectra*, pp. 100-102, Nov. 2003
9. T. Lulé, S. Benthien, H. Keller, F. Mütze, P. Rieve, K. Seibel, M. Sommer, M. Böhm, "Sensitivity of CMOS based imagers and scaling perspectives," *IEEE Trans. Electron Devices*, vol. 47, no. 11, pp. 2110-2122, Nov. 2000.
10. Eric R. Fossum, "CMOS image sensors combat noise," *EE Times*, May 2003.

## Biographies

**Hans Wach** received his B.S. degree in 1996 and a Ph.D. in 2000 both in Electrical and Computer Engineering from the University of Colorado. Since 2002 he has worked as a senior systems engineer at CDM Optics designing color imaging systems that use Wavefront Coding technology.

**Edward R. Dowski, Jr.** received his BS in Electrical Engineering from the University of Rhode Island, Kingston and his Ph.D. in Optics and Signal Processing from the University of Colorado, Boulder. After developing Wavefront Coding technology in 1995 he is one of the founders of CDM Optics and now serves as the Vice President of the company.